International Journal of Nanomedicine

Dovepress
Taylor & Francis Group

Open Access Full Text Article

ORIGINAL RESEARCH

Melatonin-Loaded Sacchachitin Nanofiber Hydrogel as a Novel Non-Steroidal Platform for Atopic Dermatitis Therapy

Chien-Ju Lin[1], Bang-Yu Wen[2], Yu-Kai Liang[3], Wen-Chen You[4], Hsiu-O Ho[5], Ming-Thau Sheu[6], Hong-Liang Lin[1,7], Ling-Chun Chen[2]

[1]School of Pharmacy, College of Pharmacy, Kaohsiung Medical University, Kaohsiung, Taiwan, Republic of China; [2]Department of Biotechnology and Pharmaceutical Technology, Yuanpei University of Medical Technology, Hsinchu, Taiwan, Republic of China; [3]Department of Pharmacy, Chia-Nan University of Pharmacy and Science, Tainan, Taiwan, Republic of China; [4]Division of Medical Devices and Cosmetics, Taiwan Food and Drug Administration, Ministry of Health and Welfare, Taipei, Taiwan, Republic of China; [5]School of Pharmacy, College of Pharmacy, Taipei Medical University, Taipei, Taiwan, Republic of China; [6]Panion & BF Biotech Inc., Taipei, Taiwan, Republic of China; [7]School of Pharmacy, College of Pharmacy, National Defense Medical University, Taipei, Taiwan, Republic of China

Correspondence: Hong-Liang Lin; Ling-Chun Chen, Email hlglin@mail.ndmctsgh.edu.tw; d8801004@mail.ypu.edu.tw

Introduction: Atopic dermatitis (AD) is a chronic inflammatory skin disease commonly managed with topical corticosteroids or calcineurin inhibitors, which may raise concerns with long-term use. Safe, non-steroidal topical therapies capable of restoring skin barrier function while modulating local immune responses remain limited.

Methods: A sacchachitin nanofiber (SCNF)-based hydrogel incorporating melatonin (MSC) was developed and evaluated for physicochemical properties, stability, and therapeutic efficacy using a 2,4-dinitrochlorobenzene (DNCB)-induced NC/Nga mouse model of AD. Clinical scores, histological features, and immunological biomarkers were assessed.

Results: Among the tested formulations, the melatonin-loaded hydrogel (MSC) demonstrated the most pronounced therapeutic efficacy compared with other formulations, significantly reducing AD severity, epidermal hyperplasia, mast cell infiltration, and Th2-associated markers including IgE, IgG1, and IL-4. Melatonin remained chemically stable for at least 31 days and did not compromise hydrogel mechanical or adhesive properties. In this system, sacchachitin nanofibers primarily function as a structural scaffold, whereas melatonin provides the principal biological and immunomodulatory activity.

Conclusion: The melatonin-loaded SCNF hydrogel represents a promising non-steroidal and biocompatible topical platform for AD. In this system, SCNF primarily serves as a structural scaffold, whereas melatonin provides immunomodulatory and anti-inflammatory activity. These findings support further translational investigation.

Keywords: atopic dermatitis, sacchachitin nanofibers, melatonin, hydrogel, NC/Nga mice

Introduction

Atopic dermatitis (AD) is a chronically recurring inflammatory skin disease that affects up to 20% of children and 3% of adults worldwide and displays increased prevalence in industrialized regions.[1,2] Characterized by intense pruritus, skin barrier dysfunction, and immune dysregulation, AD presents a significant burden on patients' quality of life due to its persistent symptoms and associated comorbidities such as asthma, allergic rhinitis, and food allergies.[3,4] The disease often initiates with xerosis and erythematous, eczematous lesions primarily on the flexural surfaces, progressing to chronic lichenification due to repeated scratching.[5] Recent studies have revealed that AD results from the multifactorial interaction between genetic factors, environmental exposures, immune dysregulation, and microbiome imbalance.[6] Mutations in the filaggrin gene, crucial for skin barrier integrity, are strongly associated with early onset and severe forms of AD.[7] Additionally, dysbiosis of skin microbiota, particularly overgrowth of Staphylococcus aureus, exacerbates inflammation and impairs the recovery of skin barrier function.[8]

https://doi.org/10.2147/IJN.S574853
Received: 17 November 2025
Accepted: 11 February 2026
Published: 17 February 2026

Traditional therapies primarily rely on topical corticosteroids and calcineurin inhibitors. While these treatments are effective in symptom control, they often pose long-term risks such as skin atrophy and systemic immunosuppression.[9] Emerging systemic therapies, such as biologics targeting interleukin-4 and −13 (eg, dupilumab), JAK inhibitors, and PDE4 inhibitors, have shown promise. However, these treatments are often costly, require medical supervision, and may be unsuitable for children or patients with mild-to-moderate disease.[10–12] Therefore, there is a growing need for safe, accessible, and non-steroidal alternatives.

Melatonin, a neurohormone best known for regulating circadian rhythms, also possesses potent anti-inflammatory, antioxidant, and immunomodulatory effects.[13] In AD, melatonin not only reduces sleep disturbances, a common symptom exacerbating disease severity, but also modulates Th1/Th2 immune balance and reduces oxidative stress in skin tissues[14] A randomized clinical trial has demonstrated that oral melatonin improved both sleep onset latency and eczema severity in children with AD.[15]

In recent years, significant progress has been made in developing targeted immunotherapies for AD. The IL-4Rα antagonist dupilumab became the first biologic approved for moderate-to-severe AD, showing substantial clinical improvement with a favorable safety profile.[16] Other monoclonal antibodies, such as tralokinumab (anti–IL-13) and lebrikizumab, offer additional therapeutic options.[17] Moreover, Janus kinase (JAK) inhibitors, such as upadacitinib, abrocitinib, and baricitinib, target multiple cytokine pathways and provide rapid symptom relief.[18,19] However, while these therapies have demonstrated efficacy, their use may be limited by systemic side effects (eg, conjunctivitis and other infections), high costs, long-term safety uncertainties, and accessibility challenges in low-resource settings.[20]

Parallel to pharmacological advances, natural biomaterials have drawn increasing attention for their regenerative potential. Sacchachitin, a fungal-derived biopolymer rich in β-1,3-glucan and chitin, exhibits excellent biocompatibility, moisture retention, and wound-healing properties.[21] When processed into Sacchachitin nanofibers (SCNF), its surface area, porosity, and drug-loading capacity are enhanced, making it an attractive scaffold for topical delivery systems. Previous studies have demonstrated that SCNF hydrogels promote fibroblast proliferation, collagen synthesis, and anti-inflammatory responses in wound models.[22] Compared to immunotherapy, the SCNF-based hydrogel system offers several key advantages: 1) it enables localized, sustained release with minimal systemic exposure; 2) it can serve as a steroid-free alternative suitable for long-term use, including in pediatric settings, 3) it is cost-effective and scalable; and 4) it exhibits favorable physical properties, biocompatibility, and storage stability.

It was hypothesized that incorporating melatonin or bioactive matrices such as an ultrasound-decellularized extracellular matrix (UdECM) into SCNF-based hydrogels could further enhance their therapeutic properties by offering sustained drug release and synergistic effects on tissue repair. UdECM has been shown to retain critical ECM components such as collagen and glycosaminoglycans, which are essential for restoring the structural and immunological balance of damaged skin.[23] As a result, we developed and evaluated several SCNF-based hydrogel formulations, including MSC (melatonin-loaded), USC (UdECM-loaded), and TSC (TEMPO-oxidized) in this study. These SCNF-based hydrogel formulations were assessed for their physical properties, drug stability, and therapeutic efficacy in a 2,4-dinitrochlorbenzene (DNCB)-induced NC/Nga mouse model of AD. The goal was to explore the feasibility of using these hydrogels as a non-steroidal, biocompatible platform for improving AD symptoms through both barrier repair and immune modulation.

Materials and Methods

Materials

Transcutol® HP was supplied by Gattefossé (ELGIN, France). Acetic acid, citric acid, formic acid, sodium dodecyl sulfate, sodium chloride, sodium hydroxide, coomassie blue R-250, 10X phosphate-buffered saline, glycerol, 2,4-dinitrochlorobenzene, Tween 20, sodium dihydrogen phosphate, and sulfuric acid were purchased from Sigma–Aldrich (St. Louis, MO, USA). Natrosol®250 (water-soluble hydroxyethylcellulose, HEC) was purchased from Hercules (Passaic, New Jersey). Melatonin was purchased from Swati Spentose Pvt. Ltd. (Gujarat, India), and attane (isoflurane) was purchased from Panion & BF Biotech Inc. (Taipei City, Taiwan). Production of sacchachitin (SC) hydrogel and TEMPO-oxidized sacchachitin (TEMPOSC050) followed the procedure as reported by Chao et al.[22] Acetonitrile (HPLC

grade) and methanol (HPLC grade) were supplied by LiChrosolv® (Merck, Germany). Protease inhibitor cocktail (EDTA-Free, 100X in DMSO, #K1010) was purchased from APExBIO (Houston, USA). IgE Mouse Uncoated ELISA Kit (Invitrogen, #88-50460-88), IgG1 Mouse Uncoated ELISA Kit (Invitrogen, #88-50410-88), and IgG2a Mouse Uncoated ELISA Kit with Plates (Invitrogen, #88-50420-22) were purchased from Thermo Fisher Scientific (Waltham, USA). Mouse Interleukin 4 (IL4) ELISA kit (SEA077Hu) was purchased from USCN Business CO., Ltd. (Wuhan, Hubei, China). HEC polymer is a partially substituted poly(polyhydroxyethyl) ether of cellulose, which is formed by the polysaccharide cellulose and its (1,4)-linked D-glucose units. HEC used in this study has a MS (total substitution) of 2.5 (10 ethylene oxide groups/4 anhydroglucose unit) and a DS (degree substitution) of 1.5 (6 hydroxyls substituted/4 anhydroglucose units). HEC used in this study was a pharm grade and has a weight average molecular weight (Da) 1,000,000 and Brookfield LVF viscosity at 25 C is 1,500–2,500 mPas (at 1% solution concentration).

Methods

HPLC–UV/Vis Method Development and Validation for Quantitative Analysis of Melatonin

An HPLC–UV/Vis system (Jasco, Tokyo, Japan) comprised an RHPLC pump (PU-4180), an RHPLC autosampler (AS-4150), and a UV-570 UV/Vis detector was employed to quantify melatonin concentration. SISC version 3.1 (Scientific Information Service Co., LTD., Taipei, Taiwan) was used as the data processing system. The column (Inertsil® ODS-3 4.6×150 mm, 5 μm, GL Sciences) was equilibrated at a temperature of 30 ± 2 °C with a mobile phase composed of acetonitrile/3.7 mM KH2PO4 (pH 3.5) at a volume ratio of 25:75, using a flow rate of 1.0 mL/min. The injection volume was 10 μL and the detection wavelength was 222 nm. The detection wavelength of 222 nm was selected based on preliminary specificity testing, which showed no detectable interference from hydrogel excipients under the applied chromatographic conditions.

The HPLC analysis method was validated through intraday and interday trials, each performed in triplicate for each concentration. The results were calculated using a linear regression method, and the integrated peak area was applied to the linear regression equation to evaluate the concentration of melatonin and the precision and accuracy of the analysis method. The linear regression equation was required to have a correlation coefficient (R^2) greater than 0.995. For each concentration, the coefficient of variation (CV) for precision and the relative standard error (RSE) for accuracy were required to be below 5%.

Production of Sacchachitin Nanofibers (SCNFs) and TEMPO-Oxidized SCNFs

The production of SCNFs and TEMPO-oxidized SCNFs was performed as reported previously.[22] Briefly, hot water-extracted Ganoderma fibers (50 g) were digested with 400 mL 1 N NaOH for 24 h at 85 °C. After digestion, the residue was collected and washed with deionized water to remove any residual NaOH. H_2O_2, applied at a m/v ratio of 3:1 based on the residue mass, was then used for depigmentation. After bleaching, the pulp mixture was washed thoroughly with double-distilled water (ddH_2O). The pulp, referred to as the SC fiber, was collected through filtration and then lyophilized. The composition of SC fiber produced using this method has previously been determined to be 40% chitin and 60% β-1,3-glucan24. Two different SCNFs were fabricated using either mechanical disintegration or chemical TEMPO-oxidization. In mechanical treatment, 4 g of the SC fiber was dispersed into 200 mL ddH_2O and homogenized with Polytron® PT 3100D (Kinematica AG, Bohemia, NY, USA) at 10,000 rpm for 5 min, followed by mechanical disintegration utilizing a NanoLyzer® N-2 (Hsinchu, Taiwan) microfluidizer under 20,000 psi for ten cycles. After microfluidization, the SCNF suspension became a gel form, giving rise to the SCNF hydrogel. For the chemical treatment method that utilized TEMPO-oxidation, 5 g of SC fiber was suspended in 375 mL ddH_2O containing 0.0625 g TEMPO (98%, Alfa Aesar, Ward Hill, MA, USA) and 0.625 g sodium bromide. The TEMPO-mediated oxidation of the SC fiber slurry was initiated through the addition of 5% NaClO (aq) up to a final concentration of 5.0 mmol/g SC with continuous stirring at room temperature. To maintain a pH = 10 throughout the reaction, 5 N NaOH or 1 N HCl was added accordingly for 2 h or until no further change in pH was observed. The oxidation reaction was quenched with 5 mL of ethanol, followed by 200 mL of acetone to precipitate the TEMPO-oxidized SCNF. The TEMPO-oxidized SCNF slurry was dialyzed with OrDial® D80 (MWCO: 60008000) for seven days in ddH_2O at room temperature. The dialyzed slurry

was further homogenized using a microfluidizer under 20,000 psi for one cycle and then lyophilized. The oxidized SCNFs are hereafter referred to as T050SC.

Chemical Characterization of One-Pot Fabricated Sacchachitin (SC)

Chemical characteristics of one-pot fabricated SC used for the preparation of Sacchachitin Nanofibers (SCNFs) hydrogel, including sugar components, sugar skeleton analysis, and protein analysis and total nitrogen content, were performed followed the same procedure as that reported by Su et al.[24]

Physical and Chemical Characterizations of Mechanically Disintegrated SCNF and Chemically TEMPO-Oxidized SCNFs

Physical characteristics including Fourier-transformed infrared (FT-IR) spectra, ^{13}C cross-polarized magic-angle spinning (CP-MAS) nuclear magnetic resonance (NMR) spectra, x-ray diffraction (XRD) spectra, determination of the size and zeta potential (ζ), evaluation of the gel-forming properties, transmission electronic microscopy (TEM), scanning electronic microscopy (SEM), water-retention ability, and the carboxylate and aldehyde contents of T033SC were measured followed the same procedures as those reported by Chao et al.[22]

Sacchachitin Nanofiber-Based (SCNF-Based) Hydrogel Formulation

A mixture of 110 g of SCNF hydrogel, obtained using the above procedure, comprised a Sacchachitin fiber concentration of 2.5%, 0.3 g of HEC and 5% glycerol was dried in an oven at 40 °C for 8 h to form Sacchachitin films. Thereafter, the Sacchachitin films were combined with three different amounts of HEC (1%, 2.5%, and 5%), separately placed in a cantilever mixer at 25 °C and subjected to blending at 800 rpm until homogeneous. The SCNF-based hydrogels obtained through this method are referred to as 99SC, 97.5SC, and 95SC, respectively, corresponding to the addition of 1.0%, 2.5%, and 5.0% of HEC.

Morphological Examination

After lyophilization of the three different SCNF-based hydrogels (99SC, 97.5SC, and 95SC), the samples were gold-plated with a gold-plating machine and then observed using a scanning electron microscope (SU3500 Hitachi, Tokyo, Japan). Differences in the surface type, internal pores, and pore sizes of the SCNF-based hydrogels were examined.

Texture Analysis Studies: Adhesion Test and Compression Test

Adhesion testing of the SCNF-based hydrogel scaffolds was performed using an XT plus Texture Analyzer (Stable Micro Systems, UK) equipped with a 5 kg weighing sensor. For each measurement, 0.5 g of the degassed sample was placed on the lower panel. The probe descended at a constant speed (10 mm/s) until it contacted the sample and applied a force of 1 N, which was maintained for 30s, after which the probe was retracted at the same constant speed. Force–time curves were generated for each measurement using an average of three replicates.

An XT plus texture analyzer was also utilized to perform a compression test on the fabricated SCNF-based hydrogel scaffolds to evaluate their hardness, compressibility, viscosity, and cohesion. The samples were placed in a 5 mL centrifuge tube and centrifuged to remove air bubbles. They were then placed under a 10 mm analytical probe, which descended at a constant speed (1 mm/s) until it contacted the sample and applied a trigger force of 300 g, before retracting at the same constant speed. Force–time curves were generated for each measurement using an average of three replicates.

In vivo Animal Studies of Atopic Dermatitis

Preparation of SCNF-Based Hydrogel Scaffolds for Animal Testing

The SCNF-based hydrogel 97.5SC was used as the control and was designated SCH. Another three SCNF-based hydrogel scaffolds were prepared to yield melatonin, UdECM, and T050SC hydrogels, designated MSC, USC, and TSC, respectively. MSC, USC, and TSC were formulated by mixing 1 g of either 4% melatonin in Transcutol, 1 g 10% UdECM, or 1g 10% T050SC with 1g 97.5SC SCNF-based hydrogel to give final concentrations of 4%, 10%, and 10%, respectively. The prepared hydrogels were then used for in vivo animal studies. UdECM was prepared as per a previous study.[25] An XT plus Texture Analyzer was used to conduct the texture analysis of adhesion and compressibility for all

four SCNF-based hydrogel scaffolds (SCH, MSC, USC, and TSC). The uniformity and stability of melatonin in MSC hydrogels were also evaluated.

Animal Study

All animal procedures were conducted in accordance with institutional guidelines for the care and use of laboratory animals and adhered to the AVMA Guidelines for the Euthanasia of Animals (2020). All animal experiments were reviewed and approved by the Animal Care and Use Committee of Taipei Medical University (protocol number: LAC-2021-0024), ensuring compliance with the Animal Protection Law and relevant regulations. NC/Nga mice (male, 16–23 weeks old) were provided by Professor Mei-Jin Chen of National Cheng Kung University (Tainan, Taiwan, ROC). The mice were housed at the Taipei Medical University Animal Center in a third-level, specific-pathogen-free (SPF), independent air-conditioned room. The temperature was maintained at 24–27 °C, and the humidity was maintained at 60%–70%. The mice had free access to aseptic standard feed and drinking water and were exposed to a 12-h automatic light/dark cycle. The experiment was only carried out once the mice had acclimatized to the environment to ensure a stable physiological and psychological state. Fasting and water deprivation was not required before drug administration. Body weight, behavior, diet, bowel movements, activity, and adverse reactions were recorded throughout the experiment.

Induction of Atopic Dermatitis (AD) Lesions on NC/NGA Mice

NC/Nga mice were originally established as inbred strains of Japanese fancy mice. Under normal conditions, NC/Nga mice develop spontaneous skin lesions, which are characterized by high concentrations of total immunoglobulin E (IgE) and inflammatory cells in plasma that invade the skin. NC/Nga mice affected by foreign allergens begin to scratch their face, ears, mouth, and back with their hind paws, causing severe skin damage. All these features are similar to those found in clinical patients with AD, so NC/Nga mice are considered the most suitable model for human atopic dermatitis.

Skin lesions due to AD were induced on the dorsal region of the NC/NGA male mice one week prior to the start of the experimental trial using DNCB according to the experimental schedule as shown in Figure S1. Briefly, the 16–23-week-old NC/NGA male mice were anesthetized using a gas anesthesia machine with isoflurane (which conformed to the American Veterinary Medical Association (AVMA) Guidelines for the Euthanasia of Animals (2020), and a 6 cm long × 3.5 cm wide patch was shaved on their dorsal skin. DNCB was dissolved in acetone/olive oil (3:1, v/v) to prepare 1% and 0.4% solutions. On day one, 150 μL of 1% DNCB was applied to the shaved dorsal area and 50 μL of 1% DNCB was applied to both ears of the mice. On day 5, the same volumes were applied using 0.4% DNCB (illustrated in Figure S1 (A)). Prior to DNCB application, 200 μL of blood was collected from the facial vein by trained personnel to minimize distress. Whole blood was centrifuged at 6000 rpm for 10 min at 4 °C to obtain plasma. Total plasma IgE levels were quantified using a Mouse IgE Uncoated ELISA Kit to confirm successful induction of AD in each mouse.

Atopic Dermatitis Wound Evaluation

Atopic Dermatitis Treatment Trials

As shown in Figure S1 (B), six experimental groups were established (n = 4 mice per group): a negative control, DNCB-induced control (AD control), sacchachitin-based hydrogel-treated (SCH), USC hydrogel-treated (USC), MSC hydrogel-treated (MSC), and TSC hydrogel-treated (TSC) group. Prior to each application, the dorsal area of each mouse was shaved, blood samples were collected, and photographs were taken and scored. The plasma was separated from the blood samples by centrifugation at 6000 rpm for 10 min at 4 °C and was analyzed for IgE, IgG1, and IgG2a. For all AD-induced groups, AD was maintained by applying 150 μL of 0.2% DNCB on the dorsal ear and 50 μL on both ears twice weekly. The AD control group received no treatment, whereas the treatment groups (SCH, USC, MSC, and TSC) received 500 mg of their respective hydrogel formulation on the dorsal skin and 25 mg behind their ears, administered five times per week for four weeks. Each hydrogel treatment was applied 30 min after the DNCB application. The skin lesions on the dorsal skin and the ears of the mice were monitored during the experiment to evaluate the therapeutic effect of the different hydrogels. The sample size (n = 4 per group) was selected based on prior NC/Nga mouse studies that demonstrated statistically significant immunological and histological differences with comparable group sizes.

On day 29, the mice were anesthetized with an intraperitoneal injection of 0.2 mL of tiletamine:zolazepam = 1:1. The depth of anesthesia was confirmed by the absence of pedal withdrawal and corneal reflexes prior to any surgical manipulation. Final photographs were obtained and scored at this stage. After achieving a verified surgical plane of anesthesia, the mice were positioned on a surgical platform and secured using a 22 G needle. Transcardial perfusion was then performed with heparinized saline at a flow rate of 12–15 mL/min until the liver visibly changed from bright red to pale. Completion of perfusion was followed by confirmation of death through the absence of heartbeat, respiration, and nociceptive reflexes, in accordance with the American Veterinary Medical Association (AVMA) Guidelines for the Euthanasia of Animals (2020). Subsequently, the heart, liver, spleen, lungs, kidneys, inguinal lymph nodes, dorsal skin, and both ears were collected, fixed in 10% neutral-buffered formalin, and stored at room temperature for further analysis.

Grading Criteria for Skin Lesions

Skin lesions were assessed using the objective Severity Scoring of Atopic Dermatitis (SCORAD) index, and the results are shown in Table S1.[26] Two independent researchers, blinded to the experimental group assignments, performed a graded assessment of the skin lesions. Before the AD induction, mice were first scored without skin damage, and twice a week after the first induction, the severity of atopic dermatitis was visually assessed, photographed, and scored. Individual scoring of skin lesion severity was based on the following six criteria: erythema, edema/papules, crusting, lichenification, superficial lesions, and dry skin, with severity ranging from 0 (none) to 1 (mild), 2 (moderate), and 3 (severe), giving a total score of 18 and with higher scores indicating higher severity of skin damage. Although SCORAD was originally developed for clinical assessment in humans, a modified version has been widely applied in NC/Nga mouse models to enable standardized evaluation of AD-like skin lesions.

Determination of Ear Injury

To assess the thickness of the epidermis layer during repeated scratching and wound healing, ear thickness was measured twice a week using a cursor caliper (Kori Seiki MFG, Tokyo, Japan).

Analysis of Plasma IgE, IgG1, and IgG2a Levels

Using the IgE, IgG1, and IgG2a Mouse Uncoated ELISA Kits, the plasma concentrations of IgE, IgG1, and IgG2a were determined. The standard samples and tested samples were prepared according to the manufacturer's instructions, and the absorbance at a wavelength of 450 nm was determined using a Cytation^{TM} 3 Cell Imaging Multi-Mode Reader (BioTek, USA). Based on the absorbance value, the concentrations of IgE, IgG1, and IgG2a were determined from interpolation from standard curves, with each sample analyzed in duplicate. Mean values were reported from these results.

IL-4 Cytokine Quantification

IL-4 cytokine levels in skin tissue were analyzed using the Mouse IL4 ELISA kit according to the manufacturer's instructions. Dorsal skin samples were cut into small pieces and 250 mg of the tissue from each sample was weighed and placed in 500 μL of PBS buffer containing 1 protease inhibitor, homogenized using ceramic beads, and centrifuged at 10,000 rpm for 5 min at 4 °C. The supernatants were aliquoted in microcentrifuge tubes and analyzed using an automated imaging system multi-function optical detector at a wavelength of 450 nm. The mean value was obtained from duplicates of each sample.

Histopathological Biopsy Evaluation

On day 29, the dorsal skin and ear tissues of the mice were removed and fixed with a 10% formaldehyde fixative solution and stored at room temperature. Thereafter, the tissues were entrusted to Tuosheng Technology Co., Ltd. for paraffin-embedding and slice processing. Tissue section staining was performed using hematoxylin and eosin (H&E) and toluidine blue (TB). After mounting, the skin tissue was observed after hydrogel treatment using light microscopy (BX43, Olympus, USA). H&E was used to assess the degree of epidermal hyperplasia, while TB was used to quantify mast cells.

Statistical Analysis

Statistical analysis was performed by one-way or two-way ANOVA and Bartlett's statistical correction. Statistical significance was defined as $p < 0.05$, with *: $p < 0.05$; **: $p < 0.01$; and ***: $p < 0.005$ indicating increasing levels of significance.

Results

HPLC Analysis and Validation for Determination of Melatonin Concentration

Melatonin content was analyzed qualitatively and quantitatively using HPLC/UV analytical methods. Standard solutions of 0.01, 0.02, 0.04, 0.08, and 0.10 mg/mL of melatonin were prepared for intraday and interday validation. As shown in Figure S2, melatonin retention time (R.T.) was found to be 5.9 min using this method. The validation of precision and accuracy for intraday and interday is shown in Figure S3 (A) and S3 (B), respectively. The linear regression equation of the calibration curve for intraday and interday was found to be y = 69,525,106.8519x – 107,025.2759 and y = 57,909,536.1759x – 45,935.4088, respectively, with both R^2 values being greater than 0.995. Acceptable precision and accuracy were found for both intraday (CV, 0.244–2.902%; RSE, –1.740–1.991%) and interday (CV, 0.014–1.9619%; RSE, –1.883–2.000%), with CV and RSE being less than 5% for both methods. Overall, the HPLC method used in this analysis demonstrated good sensitivity and reproducibility for melatonin and was suitable for both qualitative and quantitative analysis.

Chemical Characterization of One-Pot Fabricated SCNF

The chemical characterization of one-pot fabricated SCNF followed the same procedures as that reported by Su et al.[24] Results of chemical characterizations could refer to that reported in the corresponding study by Su et al.[24] The chemical characteristics of one-pot fabricated SCNF were concluded as the following. The main constituents of sugar component in one-pot fabricated SC were confirmed to be glucose and N-acetylglucosamine by analyzing the acid-treated hydrolyte from one-pot fabricated SC. The acetylation products of the hydrolyte determined by GC analysis were also demonstrated to be these two ingredients of β-1,3 glucan and N-acetylglucosamine to be at a ratio of 60% to 40%. Measurement of the protein content of one-pot fabricated SC produced no colour reaction, implying that one-pot fabricated SC contains virtually no protein. The total nitrogen content was determined to be 3.5%, which is equivalent to the total nitrogen content of N-acetylglucosamine, further confirming that the cell wall of Ganoderma mycelia was principally composed of the β-form of glucan and poly (N-acetylglucosamine) as a form of Chitin-β-glucan complex at a polysaccharide/chitin ratio of 60/40.

Physical and chemical characterization of mechanically disintegrated SCNF hydrogels and chemically TEMPO-oxidized SCNFs (T050SC) with one-pot fabricated SCNF

Mechanically disintegrated SCNFs and chemically TEMPO-oxidized SCNFs (T050SC) were prepared using the one-pot fabrication method and designated as SCNFs and T050SC, respectively. The particle size of the T050SC nanofibers was determined by dynamic light scattering (DLS), revealing an average fiber diameter of 436.4 ± 27.7 nm (Figure S4). This confirms that the nanofibers remain in the nanoscale range suitable for hydrogel formation and potential drug delivery applications. Physical characteristics including by FTIR (Figure S5), cross-polarized magic-angle spinning (CP- MAS) 13C ssNMR (Figure S6), and x-ray powder diffraction (Figure S7) were measured following the same procedures as reported in a previous publication.[22] Those results with refer to this publication are summarized as follows. FTIR spectra of both T050SC and SCNFs showed representative cellulosic or chitin peaks, ie, O–H, C–H, and C–O stretching vibrations at 3400, 2900, and 1060 cm^{-1}, respectively. After oxidation, T050SC NFs exhibited a sharp peak at 1720 cm^{-1} which was C–O stretching, while the moderate C–H stretching peak at 2920 cm^{-1} had decreased. Both peak changes were attributed to transformation of $-CH_2OH$ to –COOH at C6 in the T050SC structure. 13C CP-MAS NMR spectra of SCNFs and T050SC demonstrated that both SCNFs and T050SC were mainly composed of β-1,3-glucan and chitin, and showed carbon signals for C1, C2, C3, C4, C5, and C6 located at 103, 62, 74, 87, 77, and 68 ppm, respectively. Basically, the methyl group of acetyl amide was present in the chitin structure which showed a carbon peak for C8 centered at 23 ppm. However, it was expected that the signal intensity of the C6 peak of T050SC would

accordingly decrease with oxidation of the hydroxyl group at C6. On the other hand, a new peak at 176 ppm appeared which resulted from transformation of a primary alcoholic group ($-CH_2OH$) into a carbonyl group (-C=O) by TEMPO oxidation. These alterations additionally confirmed the conversion of the C6 primary hydroxyl group to a carboxylate group. There was also a slight change in the C5 peak. C5 exhibited an upfield chemical shift from 77 to 74 ppm which overlapped with the C3 peak. This upfield shift might have been triggered by the newly created carboxylate group based on observations of the 3D structure.

Development of Melatonin Sacchachitin Hydrogel (MSC) and Characterization of Physicochemical Properties

Preparation of Sacchachitin Hydrogel

As previously described, 110 g of micronized sacchachitin liquid was homogeneously mixed with 5% glycerol and aliquoted into containers of various sizes. Samples were dried at 40 °C for 8 h and the results showed that the 400 cm^2 containers were most suitable for producing the sacchachitin film, which was easier to preserve than the liquid form and facilitated subsequent process operations.

The dried sacchachitin film was mixed with different concentrations of HEC. High concentrations of HEC (7%–10%) resulted in excessive thickening of the sacchachitin hydrogel, resulting in uneven dispersion and chipping. Therefore, lower HEC concentrations (1%, 2.5%, and 5%) were selected for subsequent experiments to allow for homogeneous mixing and these fabricated hydrogels were designated 99SC, 97.5SC, and 95SC, respectively.

Evaluation of the Physical Properties of Sacchachitin Hydrogels

Morphological Studies

The concentration and composition of hydrogel influence its stability, mechanical properties, and adhesion. To compare differences among the formulations of hydrogels with varying composition ratios, scanning electron microscopy (SEM) was performed. The results for 99SC, 97.5SC, and 95SC sacchachitin hydrogels are shown in Figure 1A–1C, respectively. SEM analysis showed that the dried form of the sacchachitin hydrogel film was porous in structure. Compared to the HEC-free sacchachitin hydrogel film, 99SC, which contained the least amount of HEC, displayed a denser and smoother morphology. The 97.5SC hydrogel displayed an even denser structure, while 95SC, which contained the highest concentration of HEC, exhibited a pronounced thickening effect resulting in a greater hardness but increased brittleness. These observations indicate that the ratio of sacchachitin:HEC directly influences the network cross-linking characteristics and properties of the hydrocolloid matrix.

Stability Test of Melatonin in the MSC Hydrogel

To evaluate stability under long-term storage, the melatonin content of the MSC hydrogels was evaluated by diluting the MSC in the mobile phase and analyzing the extract using the above validated HPLC method after 0, 1, 2, 3, 7, 10, and 31 days (n = 3). The melatonin content reduced from 99% on day 0 to 90% on day 31, thus demonstrating that melatonin in sacchachitin hydrogels maintains good stability under prolonged storage conditions.

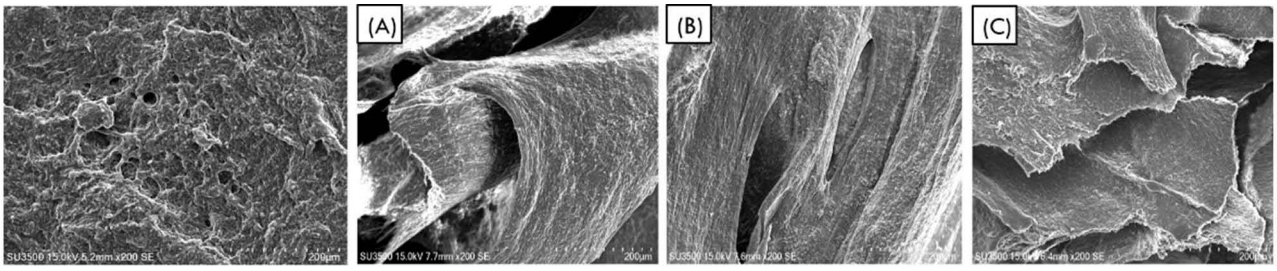

Figure 1 SEM images of hydrogel composed of sacchachitin film, (**A**) 99SC, (**B**) 97.5SC, and (**C**) 95SC surface. The samples were imaged at 200 (scale bars = 200 μm) magnification. (The SCNF-based hydrogels contained 1%, 2.5%, and 5% HEC, respectively, are referred to as 99SC, 97.5SC, and 95SC).

Texture Analysis Studies

A texture analyzer (TA.XT plus Texture analyzer, UK) was used to determine the adhesion of hydrogel matrices. In the analysis, hardness was defined as the maximum force required to compress the sample, represented as a positive peak on the force–time curve. Consistency was quantified as the area under the positive peak. Internal cohesion was obtained from the negative force measured as the probe returns to its starting position at a constant velocity, and the negative peak area formed on the force–time curve represents the viscosity. As shown in Figure 2A, increasing HEC concentration

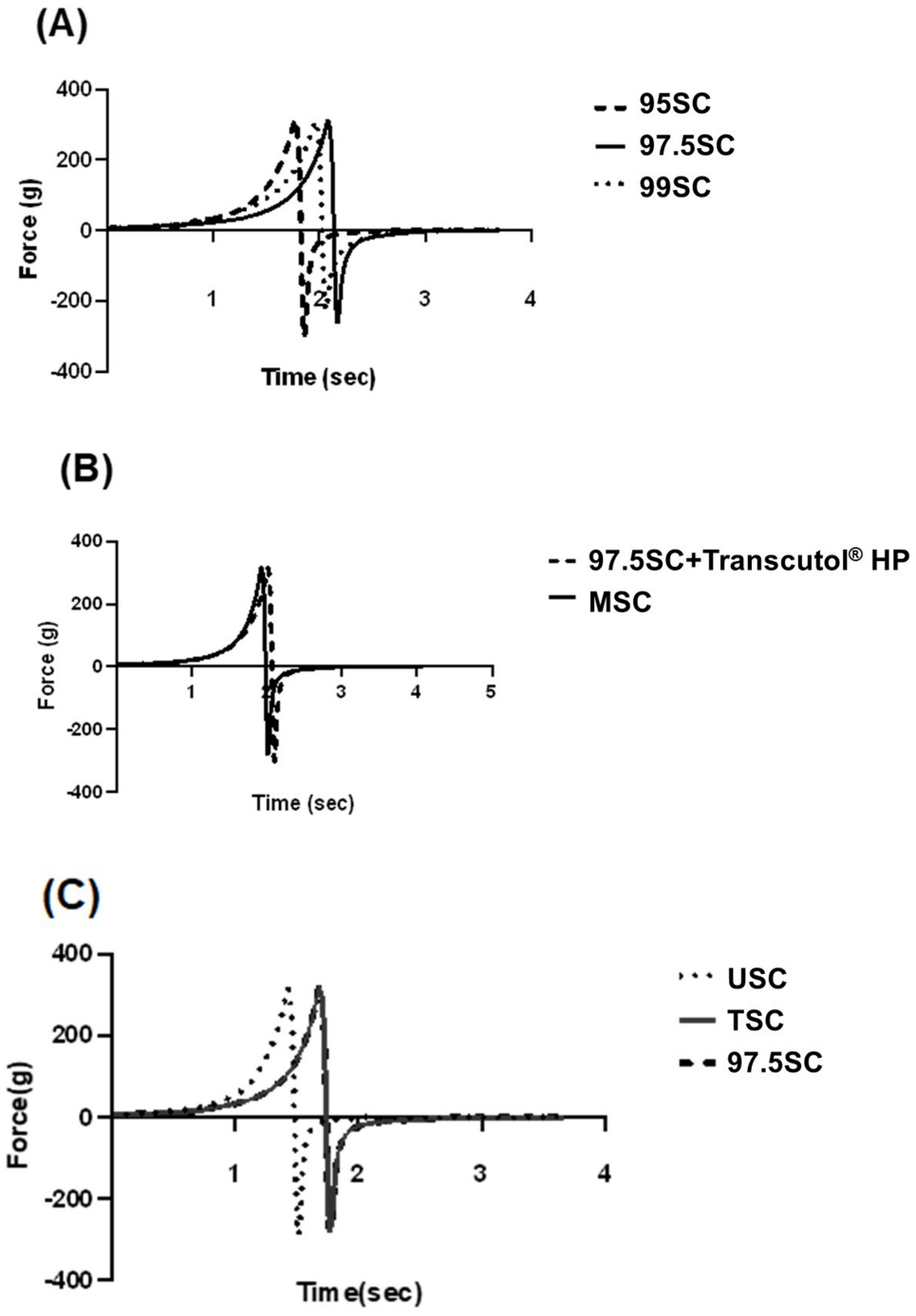

Figure 2 (**A**) Adhesion test for the sacchachitin hydrogel (**B**) Comparison of viscosity between 97.5SC and MSC containing Transcutol (**C**) Results of the compression test for USC, TSC, and 97.5SC. (The SCNF-based hydrogels contained 2.5% HEC referred to as 97.5SC.
Abbreviations: USC, USC hydrogel-treated; TSC group, TSC hydrogel-treated.

https://doi.org/10.2147/IJN.S574853

resulted in enhanced viscosity and cohesion of the 95SC hydrogel, which consequently gave greater resistance to compression by the probe and displayed greater adhesion during probe retraction. By contrast, 99SC exhibited lower viscosity and lower internal cohesion, producing a thinner, less stable structure unsuitable for forming a robust hydrogel. Therefore, 97.5SC was selected for follow-up experiments. After 97.5SC was homogeneously mixed with Transcutol and melatonin/Transcutol, respectively, the texture was analyzed again to confirm that the hydrogel texture was not altered by the incorporation of the drug. The results are shown in Figure 2B.

As shown in Figure 2C, the compression test showed that there was no significant difference in hardness, consistency, internal cohesion, and viscosity between USC, TSC, and 97.5SC. However, the USC formulation exhibited slightly lower consistency, likely due to the higher water content of UdECM, but this did not affect its viscosity. As a result, based on the combined assessment of viscosity, cohesion, and structural integrity, 97.5SC was selected as the optimal base formulation for subsequent in vivo studies.

In vivo Animal Testing in Atopic Dermatitis

This study aimed to examine the feasibility of treating AD using Sacchachitin hydrogels loaded with various biomedical materials to improve wound healing and as transcutaneous immunomodulators. An appropriate animal model was essential to assess therapeutic efficacy and therefore the NC/Nga mouse model, which closely replicates the pathological and behavioral traits of AD in humans, was selected.

Previous studies have indicated that the immune response of NC/NGA mice can vary according to age. Therefore, we obtained baseline plasma IgE levels for each mouse from their blood samples prior to AD induction to ensure comparable values across groups. In this mouse model, when the skin barrier is damaged by exogenous injury, IgE is expected to rise abnormally, with higher IgE levels correlating to a higher inflammation index. Previous studies showed that continuous administration of 1% DNCB was lethal due to high drug toxicity; therefore, 1% DNCB was only applied on days 1 and 4, and thereafter only 0.4% DNCB was applied to maintain AD status.

As shown in Figure S8, after application of 1% DNCB, the NC/Nga mice showed a gradual rise in IgE levels, displaying a IgE blood concentration of 7189 ± 0.63 ng/mL on day 4. Administration of 0.4% DNCB on days 5 and 7, increased IgE levels to 15865 ± 0.56 ng/mL. Due to the skin damage caused by DNCB, allergens invade the damaged dry skin of the NC/Nga mice, resulting in a gradual itching sensation and further skin damage caused by chronic scratching.

After measuring the blood concentration of IgE to confirm the animal model of atopic dermatitis was established, the mice were divided into six groups as described above. Shaving of the dorsal skin was performed once a week to allow for photographic observation and scoring. Blood samples were collected twice a week prior to application of DNCB to analyze for blood antibodies IgE, IgG1, and IgG2a. After blood samples were collected, 0.2% DNCB was administered to the dorsal skin and each ear to maintain the AD status and 30 min later SCH, USC, MSC, or TSC hydrogels were applied to the dorsal skin and ears of the corresponding groups. The AD control was left as the untreated control group, where only the 0.2% DNCB was applied five times a week for four weeks.

Skin lesions were assessed using an individual score based on the following six criteria: erythema (hemorrhage), edema/papules (swelling), crust (oozing), lichenification (erosion), superficial lesions, and dry skin. Each of these items was graded as 0 (none), 1 (mild), 2 (moderate), or 3 (severe) to give a total score of 18. Graded assessment of skin lesions was performed by two independent investigators. Figure 3 shows the results for the six groups of NC/Nga mice during the four-week experiment.

The results clearly show that the skin injury in the AD control group was serious and did not improve, while the MSC group showed complete wound repair and return of hair growth after four weeks. This indicates that MSC was able to effectively moisturize the skin and inhibit AD to the extent that the mice no longer showed persistent itching and scratching, indicating effective treatment of AD.

Skin lesion scores are expressed as a percentage relative to baseline values prior to treatment and the results were presented in Figure 4. It showed that,the skin lesion score was 58 ± 0.9% and 137 ± 0.1% for the MSC group and AD control group, respectively, in the first week of treatment, corresponding to a significant difference ($p < 0.0005$). The MSC group showed an 11% decrease in the skin lesion score after just one week of treatment. After two weeks of treatment, the skin lesion scores for the SCH, MSC, USC, TSC, and AD control group was 68 ± 0.9%, 56 ± 0.7%, 62 ±

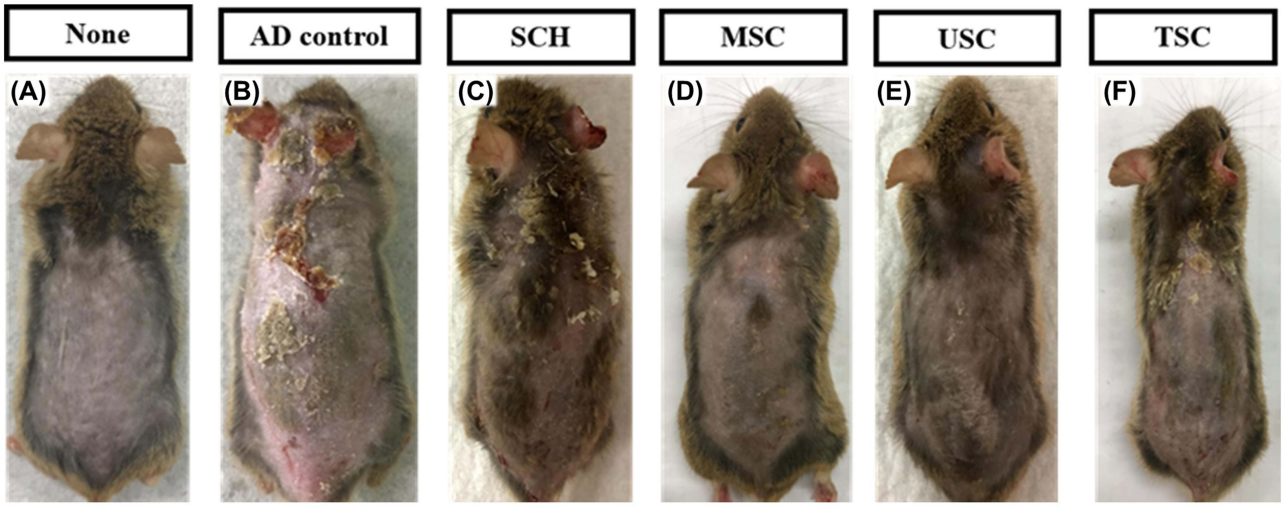

Figure 3 Representative images showing the (**A**) negative control, (**B**) AD control, (**C**) SCH, (**D**) MSC, (**E**) USC, and (**F**) TSC at the end of the four-week experiment. The AD index was evaluated by macroscopic observations.
Abbreviations: AD control, DNCB-induced control; SCH, sacchachitin-based hydrogel-treated; USC, USC hydrogel-treated; MSC, MSC hydrogel-treated; TSC group, TSC hydrogel-treated.

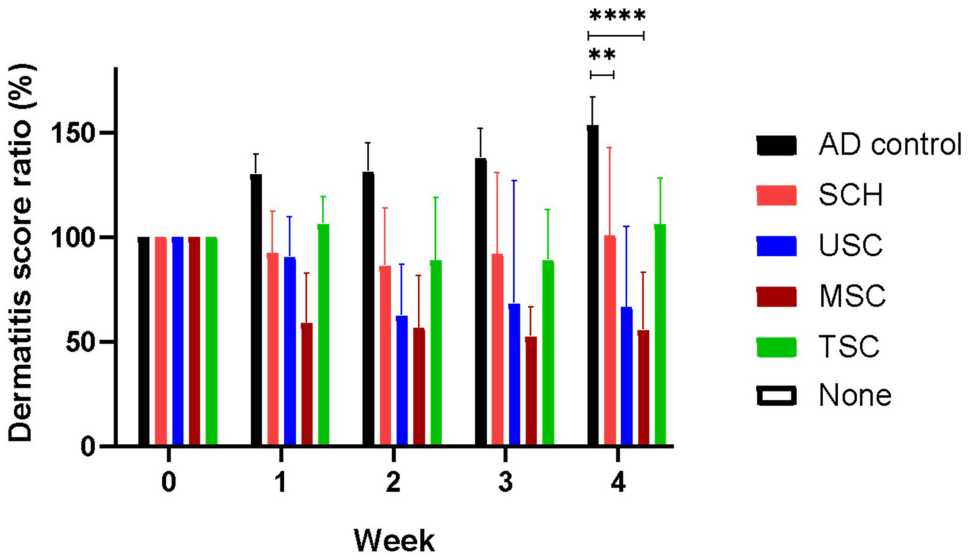

Figure 4 Improvement of skin lesions was evaluated using an AD score ratio. Data are presented as the mean ± SD (n = 4 mice/group). **: $p < 0.01$ when SCH vs AD control. ****: $p < 0.0005$ when USC, MSC, TSC vs AD control. Skin lesion scores are expressed as a percentage relative to baseline values prior to treatment.
Abbreviations: AD control, DNCB-induced control; SCH, sacchachitin-based hydrogel-treated; USC, USC hydrogel-treated; MSC, MSC hydrogel-treated; TSC group, TSC hydrogel-treated.

0.4%, 82 ± 0.8%, and 110 ± 0.6%, respectively, demonstrating a significant decrease in the skin lesion score of each group, with a further decrease of 5% seen for the SCH group in the fourth week of treatment. For the MSC group, the scores remained low (50%–60%), while the USC group score decreased to 6%, with each group displaying a significant difference compared to the AD control group ($p < 0.0005$). Studies have shown that SCH as a hydrogel carrier, can provide an antibacterial, moisturizing environment and help wound repair. Through addition of melatonin to the SCH, we observed effective penetration of the skin and inhibition of inflammation. Skin lesion scores are expressed as a percentage relative to baseline values prior to treatment.

Increased plasma IgE levels are a hallmark of immune dysregulation in AD. In this study, different hydrogel dressings were used for the treatment of AD skin lesions over the course of four weeks and blood samples were obtained from the

https://doi.org/10.2147/IJN.S574853

mice at different time points throughout the treatment period. The blood samples were analyzed for IgE, IgG1, and IgG2a concentrations. As shown in Figure 5A, the IgE blood concentrations for AD control group ranged from 24311 ± 0.6 ng/mL in the first week to 131723 ± 0.5 ng/mL in the fourth week, indicating persistent formation of wounds, skin barrier disruption, and continuous allergen penetration in the absence of treatment. This results in Th2 immune imbalance, excessive production of IgE by B cells, and the release of proinflammatory mediators, causing microvascular dilation and skin and respiratory discomfort. This excessive immune response caused by excessive IgE is referred to as a type 1 allergic reaction, also known as anaphylaxis.

After the second week of treatment, the blood concentration of IgE for all treatment groups was significantly different from that of the AD control group. Among them, the concentration of IgE in the MSC group was 22888 ± 0.5 ng/mL in week two and 43363 ± 0.5 ng/mL in week four, showing a significant reduction compared to the AD control group ($p < 0.0005$). As shown in Figure 5B, the concentrations of IgG1 for the MSC, USC, and AD control groups were 1253 ± 0.8 μg/mL, 1579 ± 0.1 μg/mL, and 2714 ± 0.1 μg/mL, respectively, demonstrating that AD-associated inflammation was significantly inhibited after the first week of treatment.

As shown in Figure 5C, the IgG2a concentration in the blood for the MSC and USC groups was 65 ± 0.3 μg/mL and 100 ± 0.4 μg/mL, respectively, whereas that for the AD control group was 175 ± 0.3 μg/mL, again showing a significant reduction ($p < 0.0005$). Conversely, the SCH and TSC hydrogel treatments did not appear to influence the blood concentration of IgG2a. These results implied that the application of SCH and TSC hydrogel on the skin could regulate the production of Th2-related antibodies (IgE and IgG1), but not the production of Th1-related antibodies (IgG2a). However, for the MSC and USC groups, inhibition of the production of both Th1- and Th2-related antibodies was observed.

After week four of the experiment, the mice were sacrificed and the dorsal skin was removed. Proteins and cytokines in the skin were extracted using a tissue grinder, and the IL-4 cytokine content was determined. As shown in Figure 5D, the IL-4 cytokine content was found to be significantly higher for the AD control group compared to all other groups. The IL-4 cytokine content of the MSC, TSC, and USC groups was found to be 7.1 ± 0.08 μg/mL, 6.7 ± 0.04 μg/mL, 6.6 ±

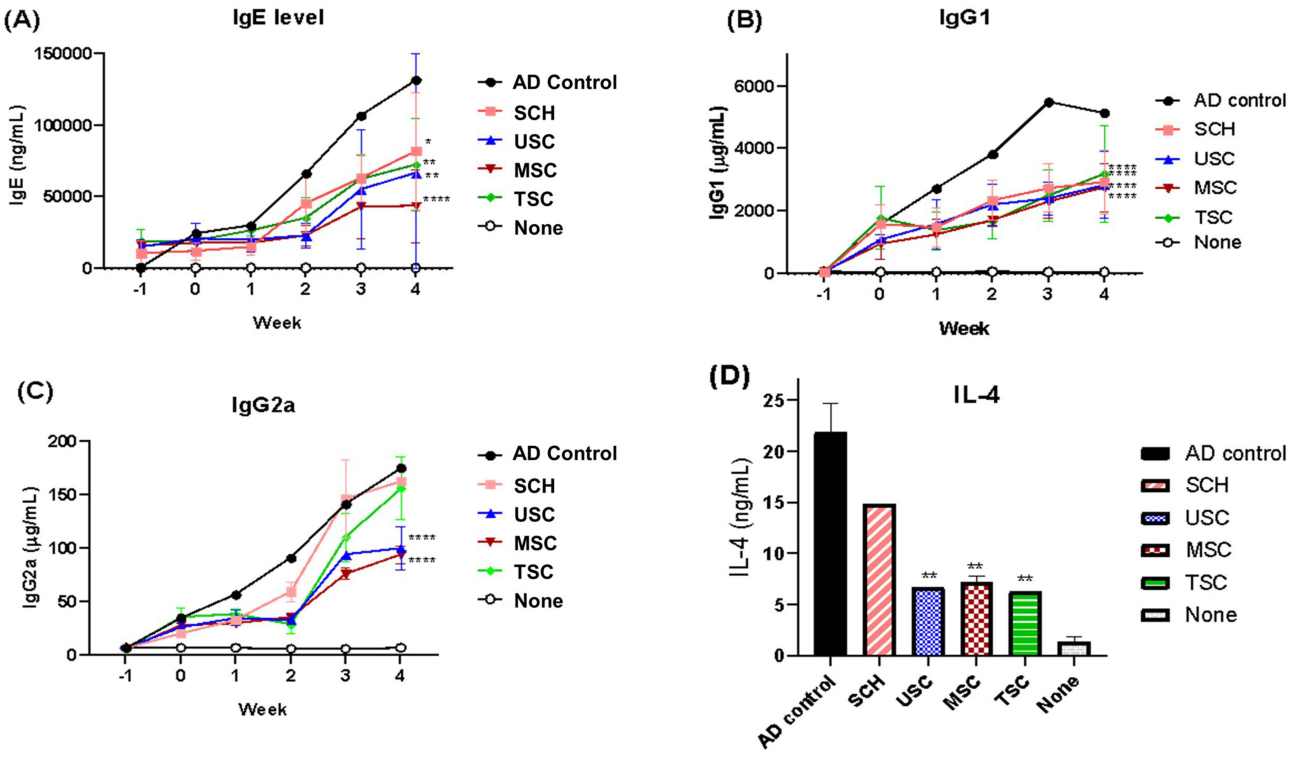

Figure 5 The plasma levels of (**A**) IgE, (**B**) IgG1, (**C**) IgG2a, and (**D**) IL-4 during the four-week experiment for the various groups. Data are presented as the mean ± SD (n = 4 mice/group). *: $p < 0.05$, **: $p < 0.01$, ****: $p < 0.0005$ compared with the AD control group.

0.07 μg/mL, respectively. These results confirm that AD drives the differentiation of T cells into Th2 cells, leading to increased production of Th2 cytokines (such as IL-4, IL-5, and IL-13), which could induce IgE synthesis and affect mast cell differentiation.

The plasma IgE, IgG1, IgG2a, and IL-4 levels for the mice are summarized in Table 1. A composite scoring system was developed based on objective treatment response and immunoglobulin/cytokine measurements. Each parameter was evaluated using a five-point scoring system. A score of 5 indicates the best treatment response in objective scoring and low IgE, IgG1, IgG2a, and IL-4 levels. A score of 1 indicates no significant treatment effect in objective scoring and high IgE, IgG1, IgG2a, and IL-4 levels. The MSC group achieved the highest overall score, confirming that MSC had the best AD treatment effect. USC treatment also demonstrated a significant treatment effect, with the objective score being high in combination with low measurement values for immunoglobulins and cytokines compared with that of the AD control. These findings further support that UdECM, when combined with sacchachitin, contributes to protecting and repairing damaged skin after application.

Based on the above results, the Sacchachitin hydrogel showed good adhesion when combined with HEC at a concentration of 2.5%. After homogenously mixing with melatonin, this was applied to the MSC mouse group to treat their induced AD. After the first week, based on the skin damage scores, there was improved skin redness and after four weeks of treatment plasma IgE, IgG1, and IgG2a levels were significantly lower compared with the untreated group ($p < 0.0005$).

In this study, we aimed to investigate whether 28 days of treatment with the prepared hydrogels could improve skin damage and inflammation caused by induced AD on the dorsal skin of mice. After the treatment period was completed, the mice were sacrificed, dorsal skin was cut, and the degree of inflammatory cell infiltration was observed by histopathological sectioning. Hematoxylin and eosin (H&E) staining was used to visualize general tissue morphology. Toluidine blue (TB) staining was performed to identify mast cells. Mast cell infiltration is mediated by IgE expression during allergic disease proliferation. When IgE expression is stimulated, mast cells will degranulate and release a variety of biologically active substances, including IL-4, IL-5 and IL-13, resulting in symptoms of allergies, including asthma and other phenomena.

Figure 6A indicates the thickness of the epidermis layer, with a black dotted line differentiating the rest of the tissue from this layer. The thickness of the dorsal epidermis layer of the mice after four weeks of treatment for the SCH, USC, MSC, and TSC groups was compared together with that for the untreated AD control group. The dorsal epidermis layer for the MSC group appeared to be thinner. The AD control group displayed epidermal hyperplasia and mast cell infiltration (red arrow in Figure 6C) consistent with typical AD symptomatic features. After quantification using ImageJ software as shown by Figure 6B, the thickness for the AD control (152 ± 0.4 μm) was confirmed to be significantly different from the that for SCH (102 ± 6.2 μm, $p < 0.005$), USC (88 ± 2.4 μm, $p < 0.0005$), MSC (49 ± 9.0 μm, $p < 0.0005$), and TSC (83 ± 3.0 μm, $p < 0.005$) groups.

TB staining confirmed the distribution of mast cells for each group. In the AD control, a dense accumulation of mast cells was observed in the dermis. This is indicative of long-term untreated skin damage, combined with repeated allergen exposure, which leads to antibody production by plasma cells. These antibodies bind to receptors on mast cells,

Table 1 Overall Assessment for Plasma IgE, IgG1, IgG2a, and IL-4 Levels

Group	Objective SCORAD	IgE	IgG1	IgG2a	IL-4	Sum
None	-	-	-	-	-	-
AD control	1	1	1	1	1	5
SCH	2	2	3	2	2	11
MSC	5	5	5	5	4	24
USC	4	4	4	4	5	21
TSC	3	3	2	3	3	14

Abbreviations: AD control, DNCB-induced control; SCH, sacchachitin-based hydrogel-treated; USC, USC hydrogel-treated; MSC, MSC hydrogel-treated; TSC, hydrogel-treated (TSC) group.

https://doi.org/10.2147/IJN.S574853

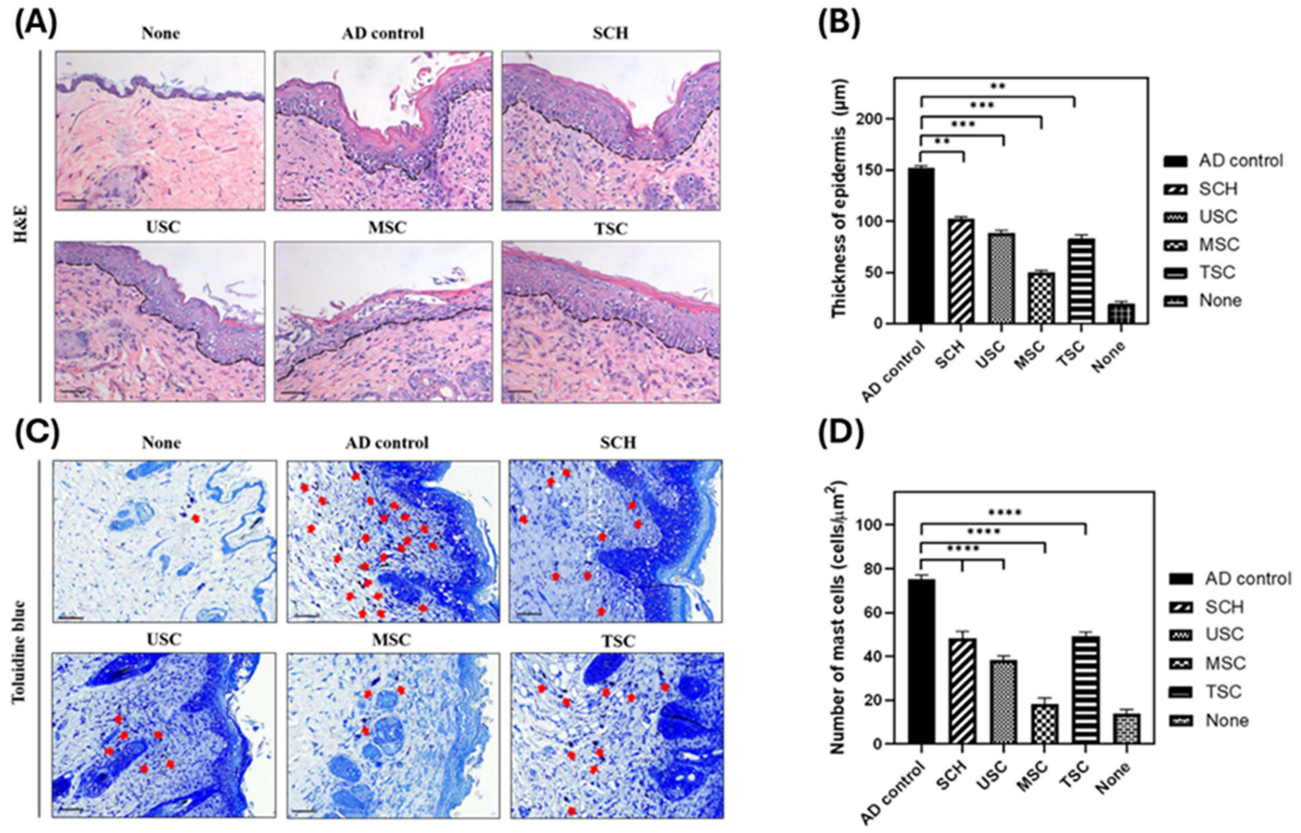

Figure 6 Histological observation of the negative control, AD control, SCH, USC, MSC, and TSC groups of NC/Nga mice. Representative dorsal skin images of histological examination (400x, scale bar = 100 μm); (**A**) H&E staining; the thicknesses of the epidermis is marked with a dotted line and (**B**) quantitative comparison of the thickness of epidermis; (**C**) toluidine blue staining, with the infiltration of mast cells indicated by arrows and (**D**) the number of infiltrated inflammatory cells (eosinophils) were measured in 1 mm2 patches of dorsal skin lesions and averaged (n = 3). The results were presented as mean ± SD (n = 4). *: $p < 0.05$, **: $p < 0.01$, ****: $p < 0.0005$ compared with the AD control group.

Abbreviations: AD control, DNCB-induced control; SCH, sacchachitin-based hydrogel-treated; USC, USC hydrogel-treated; MSC, MSC hydrogel-treated; TSC group, TSC hydrogel-treated.

triggering the release of histamine and other mediators that exacerbate allergic reactions and worsen AD symptoms. Quantification of the number of mast cells in tissue sections (as shown by Figure 6D) gave the following results for the various groups: SCH (48 ± 3.3 cells/field, $p < 0.0005$), USC (38 ± 4.4 cell/field, $p < 0.0005$), MSC (18 ± 1.6 cell/field, $p < 0.0005$), and TSC (49 ± 2.1 cell/field, $p < 0.0005$). Overall, the number of mast cells in the dermis was significantly decreased in the treated groups compared with the AD control group (75 ± 2.4 cells/field).

In addition to evaluating changes to the dorsal skin, the study also evaluated skin from the ears of the mice. The epidermal skin of the mouse ear is relatively fragile, and AD symptoms result in repeated scratching, leading to an increased itching sensation, redness, and discomfort. During this continuous cycle of chronic scratching, wounds are produced on the ear. In severe cases, damage can extend to the dermis layer, which subsequently undergoes proliferation and tissue remodeling during wound repair. Figure 7 presents the ear thickness profiles over time for the various groups. The ear thickness profiles during the four-week experimental period showed similar results to what was observed for the dorsal skin. In the AD control group, the ear thickness of mice gradually increased and by the fourth week, the mean ear thickness had reached 0.7 ± 0.08 mm, indicating a significant difference ($p < 0.005$) from that for the treatment groups: USC (0.4 ± 0.07 mm), MSC (0.3 ± 0.07 mm), and TSC (0.5 ± 0.04 mm) groups. The ear thickness of the MSC and USC groups gradually decreased during the treatment, which may be due to both these formulations being rich in type I collagen. Treatment with MSC or USC appeared to reduce itching discomfort while also effectively helping wound healing, leading to the alleviation of AD symptoms.

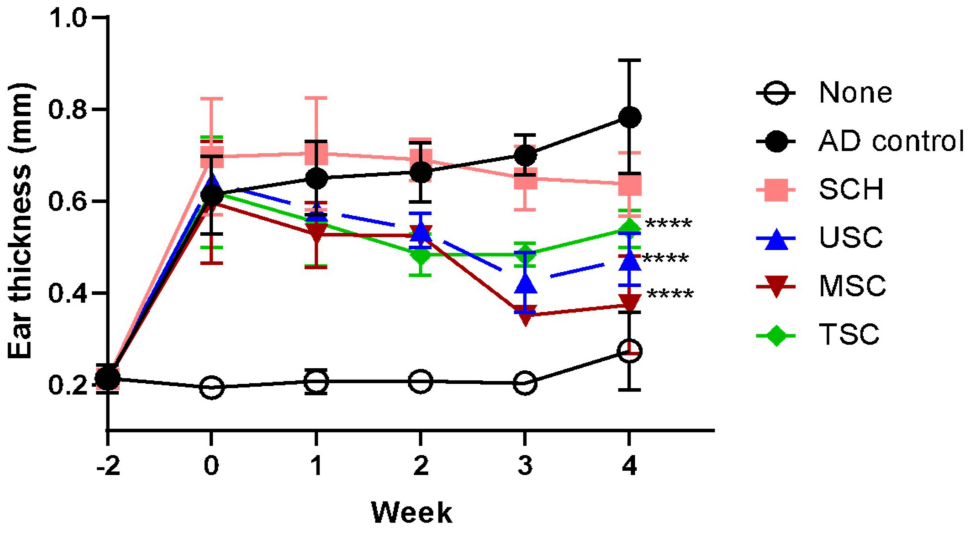

Figure 7 Epidermal thickness measurements of the ear lesions over the four week experimental period. Data are presented as the mean ± SD (n = 4 mice/group). *: $p < 0.05$, **: $p < 0.01$, ****: $p < 0.0005$ compared with the AD control group.

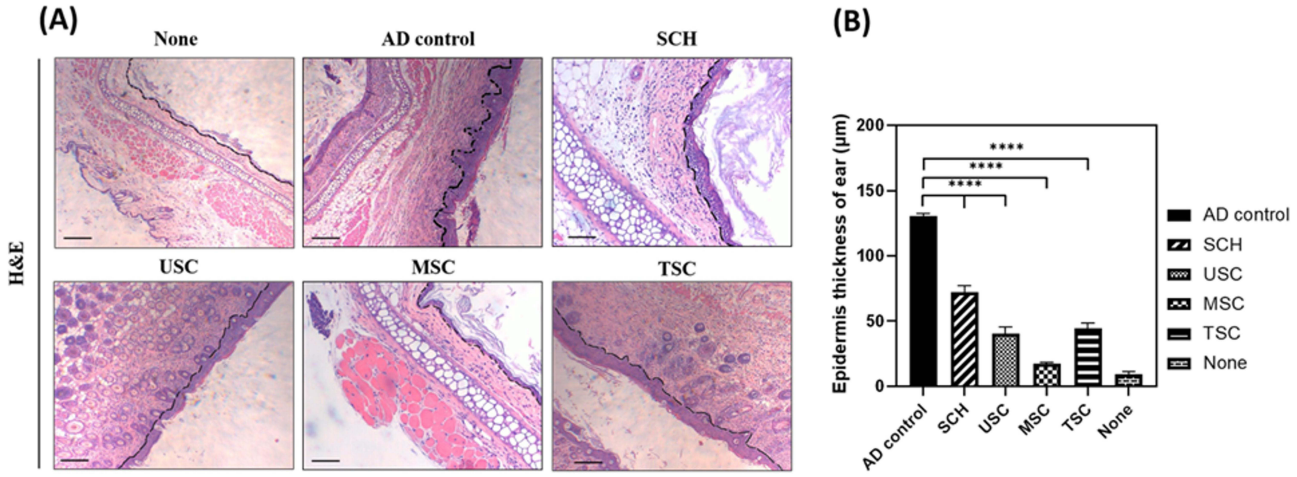

Figure 8 Histological analysis of NC/Nga mice skin samples. (**A**) Representative dorsal skin histological examination (400x, scale bar = 100 μm), The thickness of the skin after H&E dyeing is shown by the dotted line. (**B**) Quantified epidermal thickness of ear skin lesions. Data are presented as the mean ± SD (n = 4 mice/group). *: $p < 0.05$, **: $p < 0.01$, ****: $p < 0.0005$ compared with the AD control group.

To evaluate whether the various hydrogel formulations could improve skin inflammation, the dorsal skin was harvested after four weeks. As shown in Figure 8A, ear epidermal thickness and infiltration by inflammatory cells were assessed using H&E and TB staining, respectively. For the AD control group, the ear epidermal layer displayed typical features of AD epidermal thickening. The thickness of the epidermal layer was quantified using Image J analysis software and the results are illustrated in Figure 8B. Compared to the AD control group (130.6 ± 0.2 μm), all four treatment groups showed a significantly decreased thickening after four weeks of treatment: SCH, 72.1 ± 0.5 μm, $p < 0.005$; MSC, 17.1 ± 0.1 μm, $p < 0.005$; USC, 40.2 ± 0.4 μm, $p < 0.005$; and TSC, 44.5 ± 0.2 μm, $p < 0.005$. This indicates that although all treatments used in the study could aid in the repair of wounds and damaged tissues, MSC achieved the best treatment effect (17.1 ± 0.1 μm vs 130.6 ± 0.2 μm). The superior efficacy of MSC could be attributed to its ability to alleviate itching caused by the AD, resulting in less damage and redness of the epidermis caused by scratching.

https://doi.org/10.2147/IJN.S574853

Discussion

This study successfully developed a novel melatonin-loaded sacchachitin nanofiber-based hydrogel (MSC) and demonstrated its potential as a therapeutic biomaterial for the treatment of AD. Through systematic evaluations of physicochemical properties, drug stability, in vivo therapeutic efficacy, and immunomodulatory effects, the MSC hydrogel showed superior performance compared to other hydrogel formulations and untreated controls.

Regarding physicochemical characterization and structural integrity, it was found that the incorporation of HEC was crucial for optimizing the Sacchachitin hydrogel structure. Among the formulations tested, the 97.5SC hydrogel displayed the most desirable balance between viscosity, cohesion, and structural integrity. SEM analysis revealed that this formulation formed a uniform and stable porous network, which is essential for drug encapsulation and sustained release. The addition of melatonin did not compromise the mechanical properties, confirming that the MSC system maintains its textural characteristics upon drug loading.

In terms of melatonin stability and controlled release, HPLC analysis confirmed the chemical stability of melatonin in the hydrogel system over 31 days, with drug content retention exceeding 90%. This stability is critical for maintaining therapeutic efficacy during prolonged storage or use. Prior research has highlighted the antioxidative and anti-inflammatory properties of melatonin, suggesting its potential as a local therapeutic agent in skin disorders like AD25.

The NC/Nga mouse model used as an atopic dermatitis animal model in this study was used to evaluate therapeutic efficacy. This mouse model shares key features of human AD, including elevated IgE levels, barrier dysfunction, and Th2-dominant inflammation. Treatment with MSC hydrogel significantly reduced skin lesion scores, restored epidermal thickness, and improved gross skin morphology compared to both untreated controls and other hydrogel groups. Moreover, the MSC formulation notably reduced serum levels of total IgE, IgG1, and IgG2a, and decreased local IL-4 expression in lesional skin. These findings support the immunomodulatory effect of melatonin, which is known to downregulate Th2 cytokines and modulate mast cell activity.[27,28] Histological analyses further confirmed reduced mast cell infiltration and normalized epidermal thickness in MSC-treated groups, substantiating the hydrogel's role in ameliorating both cellular and structural hallmarks of AD.

Compared to other formulations prepared in this study, MSC exhibited the most pronounced therapeutic effects across all measured efficacy and immunological modulation parameters. While SCH and TSC provided mild symptomatic relief and modulated IgE and IgG1 levels, only MSC and USC significantly reduced both Th1 (IgG2a) and Th2 (IgE, IL-4) immune responses, demonstrating broader immunological benefits. These mechanisms are consistent with the observed reductions in IgE, IL-4 levels, and mast cell infiltration in MSC-treated skin. This dual immune regulation is especially valuable in AD, where both Th1 and Th2 pathways can become dysregulated in chronic stages.[29]

Regarding clinical potential and future applications, the ability of MSC to both restore skin barrier function and regulate immune response highlights its promise as a bio-based therapeutic system for AD management. Unlike conventional corticosteroids or calcineurin inhibitors, which may carry long-term side effects, the MSC hydrogel utilizes naturally derived polymers and endogenous bioactive agents with potentially reduced toxicity and improved patient compliance. However, it should be noted that topical corticosteroids and calcineurin inhibitors remain effective and safe when used appropriately according to clinical guidelines.

Future research may further explore the hydrogel's drug-release kinetics, potential for human translation, and its use in combination therapies. Additionally, its biocompatibility and structural flexibility may be leveraged for applications in other inflammatory or autoimmune skin diseases.

Conclusions

This study highlights the therapeutic potential of a melatonin-loaded Sacchachitin nanofiber hydrogel as an innovative, non-steroidal treatment for atopic dermatitis. The MSC formulation not only alleviated visible dermatological symptoms in vivo but also modulated immune response and reduced inflammatory biomarkers. Its favorable biophysical properties, biocompatibility, and drug stability make it a strong candidate for clinical translation. These results suggest that SCNF-based hydrogels, particularly those incorporating melatonin or UdECM, may serve as safe and effective alternatives to

current steroidal therapies, offering new avenues for improving patient care and quality of life in chronic inflammatory skin conditions.

Author Contributions

Chien-Ju Lin: Methodology, Formal analysis, Software, Writing – original draft, Investigation, Data curation, Visualization. Bang-Yu Wen: Methodology, Formal analysis, Software, Writing – original draft, Investigation, Data curation, Visualization. Yu-Kai Liang: Methodology, Formal analysis, Software, Writing – original draft. Wen-Chen You: Investigation, Data curation, Visualization. Hsiu-O Ho: Resources, Supervision, Validation. Ming-Thau Sheu: Resources, Supervision, Validation, Funding acquisition. Hong-Liang Lin: Conceptualization, Writing – review & editing, Project administration. Ling-Chun Chen: Conceptualization, Writing – review & editing, Project administration.

Funding

This work was supported by grants from the Kaohsiung Medical University Research Foundation (KMU-M109019, KMU-M111008, and KMU-M112028) and the National Science and Technology Council (MOST109-2320-B-037-020, MOST111-2221-E-037-004, NSTC112-2320-B-037-023 and NSTC112-2221-E-037-002).

Disclosure

The authors affirm that there are no financial or personal relationships that could be construed as having influenced the research presented in this manuscript.

References

1. Williams HC. Clinical practice Atopic dermatitis. *N Engl J Med*. 2005;352(22):2314–2324. doi:10.1056/NEJMcp042803
2. Nutten S. Atopic dermatitis: global epidemiology and risk factors. *Ann Nutr Metab*. 2015;66(Suppl 1):8–16. doi:10.1159/000370220
3. Zuberbier T, Orlow SJ, Paller AS, et al. Patient perspectives on the management of atopic dermatitis. *J Allergy Clin Immunol*. 2006;118 (1):226–232. doi:10.1016/j.jaci.2006.02.031
4. Lai-Cheong JE, McGrath JA. Structure and function of skin, hair and nails. *Medicine*. 2021;49(6):337–342. doi:10.1016/j.mpmed.2021.03.001
5. Kabashima K. Pathomechanism of atopic dermatitis in the perspective of T cell subsets and skin barrier functions – "Which comes first, the chicken or the egg?". *Dermatologica Sinica*. 2012;30(4):142–146. doi:10.1016/j.dsi.2012.07.003
6. Yang G, Vanderschueren D, Antonio L, et al. Skin barrier abnormalities and immune dysfunction in atopic dermatitis. *Int J Mol Sci*. 2020;22:21. doi:10.3390/ijms21082867
7. Palmer CNA, Irvine AD, Terron-Kwiatkowski A, et al. Common loss-of-function variants of the epidermal barrier protein filaggrin are a major predisposing factor for atopic dermatitis. *Nature Genet*. 2006;38(4):441–446. doi:10.1038/ng1767
8. Nakatsuji T, Chen TH, Two AM, et al. Staphylococcus aureus exploits epidermal barrier defects in atopic dermatitis to trigger cytokine expression. *J Invest Dermatol*. 2016;136(11):2192–2200. doi:10.1016/j.jid.2016.05.127
9. Wollenberg A, Kinberger M, Arents B, et al. European guideline (EuroGuiDerm) on atopic eczema – part II: non-systemic treatments and treatment recommendations for special AE patient populations. *J Eur Acad Dermatol Venereol*. 2022;36(11):1904–1926. doi:10.1111/jdv.18429
10. Castro M, Corren J, Pavord ID, et al. Dupilumab efficacy and safety in moderate-to-severe uncontrolled asthma. *N Engl J Med*. 2018;378 (26):2486–2496. doi:10.1056/NEJMoa1804092
11. Wollenberg A, Blauvelt A, Guttman-Yassky E, et al. Tralokinumab for moderate-to-severe atopic dermatitis: results from two 52-week, randomized, double-blind, multicentre, placebo-controlled Phase III trials (ECZTRA 1 and ECZTRA 2). *Br J Dermatol*. 2021;184(3):437–449. doi:10.1111/bjd.19574
12. Yang H, Li P, Shu H, et al. Efficacy and safety of proactive therapy with 2% crisaborole ointment in children with mild-to-moderate atopic dermatitis: a randomized controlled study. *Paediatr Drugs*. 2025;27(3):367–376. doi:10.1007/s40272-025-00682-w
13. Reiter RJ, Tan D-X, Mayo JC, et al. Melatonin as an antioxidant: biochemical mechanisms and pathophysiological implications in humans. *Acta Biochim Pol*. 2003;50(4):1129–1146. doi:10.18388/abp.2003_3637
14. Carrillo-Vico A, Lardone PJ, Alvarez-Sánchez N, et al. Melatonin: buffering the immune system. *Int J Mol Sci*. 2013;14(4):8638–8683. doi:10.3390/ijms14048638
15. Chang YS, Lin M-H, Lee J-H, et al. Melatonin supplementation for children with atopic dermatitis and sleep disturbance: a randomized clinical trial. *JAMA Pediatr*. 2016;170(1):35–42. doi:10.1001/jamapediatrics.2015.3092
16. Blauvelt A, de Bruin-Weller M, Gooderham M, et al. Long-term management of moderate-to-severe atopic dermatitis with dupilumab and concomitant topical corticosteroids (LIBERTY AD CHRONOS): a 1-year, randomised, double-blinded, placebo-controlled, Phase 3 trial. *Lancet*. 2017;389(10086):2287–2303. doi:10.1016/S0140-6736(17)31191-1
17. Pescitelli L, Rosi E, Ricceri F, et al. Novel therapeutic approaches and targets for the treatment of atopic dermatitis. *Curr Pharm Biotechnol*. 2021;22(1):73–84. doi:10.2174/1389201021666200611112755
18. Guttman-Yassky E, Teixeira HD, Simpson EL, et al. Once-daily upadacitinib versus placebo in adolescents and adults with moderate-to-severe atopic dermatitis (Measure Up 1 and Measure Up 2): results from two replicate double-blind, randomised controlled phase 3 trials. *Lancet*. 2021;397(10290):2151–2168. doi:10.1016/S0140-6736(21)00588-2

19. Bieber T. Atopic dermatitis: an expanding therapeutic pipeline for a complex disease. *Nat Rev Drug Discov*. 2022;21(1):21–40. doi:10.1038/s41573-021-00266-6
20. Sidbury R, Davis DM, Cohen DE, et al. Guidelines of care for the management of atopic dermatitis: section 3. Management and treatment with phototherapy and systemic agents. *J Am Acad Dermatol*. 2014;71(2):327–349. doi:10.1016/j.jaad.2014.03.030
21. Chuang CM, Wang H-E, Chang C-H, et al. Sacchachitin, a novel chitin-polysaccharide conjugate macromolecule present in Ganoderma lucidum: purification, composition, and properties. *Pharm Biol*. 2013;51(1):84–95. doi:10.3109/13880209.2012.711840
22. Chao FC, Wu M-H, Chen L-C, et al. Preparation and characterization of chemically TEMPO-oxidized and mechanically disintegrated sacchachitin nanofibers (SCNF) for enhanced diabetic wound healing. *Carbohydr Polym*. 2020;229:115507. doi:10.1016/j.carbpol.2019.115507
23. Aamodt JM, Grainger DW. Extracellular matrix-based biomaterial scaffolds and the host response. *Biomaterials*. 2016;86:68–82. doi:10.1016/j.biomaterials.2016.02.003
24. Su CH, Sun C-S, Juan S-W, et al. Fungal mycelia as the source of chitin and polysaccharides and their applications as skin substitutes. *Biomaterials*. 1997;18(17):1169–1174. doi:10.1016/S0142-9612(97)00048-3
25. Lin CJ, Lin H-L, You W-C, et al. Composite hydrogels of ultrasound-assisted-digested formic acid-decellularized extracellular matrix and sacchachitin nanofibers incorporated with platelet-rich plasma for diabetic wound treatment. *J Funct Biomater*. 2023;14(8):423. doi:10.3390/jfb14080423
26. Severity scoring of atopic dermatitis: the SCORAD index. Consensus Report of the European Task Force on Atopic Dermatitis. *Dermatology*. 1993;186(1):23–31. doi:10.1159/000247298
27. Kim TH, Jung J-A, Kim G-D, et al. Melatonin inhibits the development of 2,4-dinitrofluorobenzene-induced atopic dermatitis-like skin lesions in NC/Nga mice. *J Pineal Res*. 2009;47(4):324–329. doi:10.1111/j.1600-079X.2009.00718.x
28. Kim YS, Go G, Yun C-W, et al. Topical administration of melatonin-loaded extracellular vesicle-mimetic nanovesicles improves 2,4-dinitrofluorobenzene-induced atopic dermatitis. *Biomolecules*. 2021;11(10):1450. doi:10.3390/biom11101450
29. Zhang S, Yao X. Mechanism of action and promising clinical application of melatonin from a dermatological perspective. *J Transl Autoimmun*. 2023;6:100192. doi:10.1016/j.jtauto.2023.100192